

Anomalous pseudogap and superconducting-state properties of heavily disordered $Y_{1-x}Ca_xBa_2(Cu_{1-y}Zn_y)_3O_{7-\delta}$

S. H. Naqib,^{1,*} J. R. Cooper,¹ R. S. Islam,¹ and J. L. Tallon²¹*IRC in Superconductivity, University of Cambridge, Madingley Road, Cambridge CB3 0HE, United Kingdom*²*MacDiarmid Institute for Advanced Materials and Nanotechnology, Victoria University and Industrial Research Ltd., P.O. Box 31310, Lower Hutt, New Zealand*

(Received 22 December 2004; published 18 May 2005)

The role of substantial in-plane disorder (Zn) on the charge transport and ac susceptibility of $Y_{1-x}Ca_xBa_2(Cu_{1-y}Zn_y)_3O_{7-\delta}$ was investigated over a wide range of planar hole concentration p . Resistivity $\rho(T)$ for a number of overdoped to underdoped samples with $y \geq 0.055$ showed clear downturns at a characteristic temperature similar to that found at T^* in Zn-free underdoped samples because of the presence of the pseudogap. Contrary to the widely observed behavior for underdoped cuprates at lower Zn contents (where the pseudogap energy increases almost linearly with decreasing p in the same way as for the Zn-free compounds), this apparent pseudogap temperature at high Zn content showed very little or no p dependence. It also increases systematically with increasing Zn concentration in the CuO_2 planes. This anomalous behavior appears quite abruptly, e.g., samples with $y \leq 0.05$ exhibit the usual $T^*(p)$ behavior. AC susceptibility of these heavily disordered samples showed the superfluid density to be extremely low. We also discuss various possible scenarios that might lead to an anomalous Zn-induced pseudogap in the cuprates.

DOI: 10.1103/PhysRevB.71.184510

PACS number(s): 74.72.-h, 74.25.Dw, 74.62.Dh

I. INTRODUCTION

One of the most widely studied phenomena in the physics of high-temperature superconductors (HTS) is the *pseudogap phase*.^{1,2} In the presence of a pseudogap (PG), various anomalies are observed in both normal and superconducting (SC) states, which can be interpreted in terms of a decrease in the quasiparticle density of states near the chemical potential.³ Various theoretical models have been proposed to explain the origin of the PG.⁴⁻¹² But its nature remains an unresolved issue up to now.

In this paper we report systematic studies of the transport properties of $Y_{1-x}Ca_xBa_2(Cu_{1-y}Zn_y)_3O_{7-\delta}$. We have measured the dc resistivity, $\rho(T)$, room-temperature thermopower, $S[290\text{ K}]$, and ac susceptibility (ACS) of a series of sintered and c -axis-oriented crystalline films of $Y_{1-x}Ca_xBa_2(Cu_{1-y}Zn_y)_3O_{7-\delta}$ compounds with different levels of Zn, Ca, and oxygen contents. The aim of the present study was to examine the transport properties of $YBa_2Cu_3O_{7-\delta}$ (Y123) at high Zn concentration as a function of hole doping, extending from highly overdoped (OD) to underdoped (UD) states. Pure Y123 with full oxygen loading ($\delta=0$), is only slightly OD; further overdoping is achieved by substituting Y^{3+} by Ca^{2+} .^{13,14} The advantages of using Zn are (i) it mainly substitutes the in-plane Cu(2) sites, thus the effects of planar impurity can be studied and (ii) the doping level remains nearly the same when Cu(2) is substituted by Zn enabling one to look at the effects of disorder at almost the same hole concentration.^{15,16} Most of the studies on the effect of Zn on charge transport of Y123 are limited to the range of UD to optimum doping levels and at a moderate level of Zn substitution. Therefore, study of the system in the OD region with high levels of planar defects fills an important gap.

One interesting result of the present study is that, signs of a PG-like anomaly are seen clearly in overdoped

$Y_{1-x}Ca_xBa_2(Cu_{1-y}Zn_y)_3O_{7-\delta}$, but only in a highly disordered ($y \geq 0.055$) state. This PG-like feature is almost independent of oxygen deficiency δ , indicating that it is induced by disorder and not by changing the hole concentration p .

II. EXPERIMENTAL DETAILS AND RESULTS

Polycrystalline single-phase samples of $Y_{1-x}Ca_xBa_2(Cu_{1-y}Zn_y)_3O_{7-\delta}$ were synthesized by standard solid-state reaction methods using high-purity ($>99.99\%$) powders. The details of sample preparation, characterization, and oxygen annealings can be found in Refs. 13 and 14. High-quality c -axis-oriented thin films of $Y_{1-x}Ca_xBa_2(Cu_{1-y}Zn_y)_3O_{7-\delta}$ were fabricated on $SrTiO_3$ substrates using pulsed laser deposition (PLD). Details of PLD, characterization, and oxygenation of the films can be found in Refs. 14 and 17.

Various normal and SC state properties including T^* (the PG temperature) are highly sensitive to p and therefore it is important to determine p as accurately as possible. We have used the room-temperature thermopower, $S[290\text{ K}]$, which varies systematically with p for various HTS over the entire doping range extending from very underdoped to heavily overdoped regimes.¹⁸ Previous studies, following the findings of Obertelli *et al.*,¹⁸ showed that $S[290\text{ K}]$ does not vary significantly with Zn in Y123 for $\delta < 0.5$.^{16,19} Accordingly, in this doping range $S[290\text{ K}]$ is still a good measure of p even in the presence of strong in-plane potential scattering by Zn^{2+} ions. We have also calculated p for all the samples using a generalized $T_c(p)$ relation given by^{14,19,20}

$$\frac{T_c(p)}{T_c(p_{opt})} = 1 - Z(p - p_{opt})^2. \quad (1)$$

For the Zn-free samples, Z and p_{opt} take the usual, quasiuniversal values of 82.6 and 0.16, respectively,²⁰ but these pa-

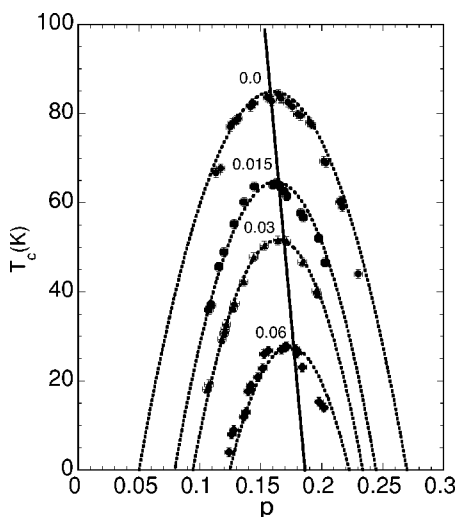


FIG. 1. $T_c(p)$ of sintered $\text{Y}_{0.80}\text{Ca}_{0.20}\text{Ba}_2(\text{Cu}_{1-y}\text{Zn}_y)_3\text{O}_{7-\delta}$. y values are shown. The straight line shows the shift in p_{opt} with Zn. In all cases p was determined from $S[290 \text{ K}]$.

rameters increase systematically with increasing in-plane disorder.^{14,19} Using p values from $S[290 \text{ K}]$ and the experimental values of T_c , a very good fit of $T_c(p)$ of the form of Eq. (1) was obtained for all the samples. Figure 1 shows the case for $\text{Y}_{0.80}\text{Ca}_{0.20}\text{Ba}_2(\text{Cu}_{1-y}\text{Zn}_y)_3\text{O}_{7-\delta}$ sintered compounds. There is a systematic shift of p_{opt} toward higher values (from $p_{\text{opt}}=0.16$ for the impurity-free case) and an increase in Z with increasing Zn content. These findings have important consequences. Increasing $Z(y)$ implies the shrinkage of the p range over which the compound is superconducting upon Zn substitution, and the shift of $p_{\text{opt}}(y)$ toward higher values implies that the superconducting dome is displaced asymmetrically toward the OD side. This latter feature,²¹ we believe, is indicative of a fundamental difference between the underdoped and overdoped regions, namely, the existence of the pseudogap in the underdoped region and its absence in the overdoped region.³ From Fig. 1 it is also seen that SC is at its strongest at $p \sim 0.186$, as this remains the last point of SC at a critical Zn concentration (defined as the highest possible Zn concentration for which SC just survives considering all the possible doping states). This has been reported earlier in other studies and the value $p \sim 0.19$ is indeed special at which the PG vanishes quite abruptly.^{3,4,14,19,21-24}

T_c was obtained from both resistivity and low field ($H_{\text{rms}}=0.1 \text{ Oe}$; $f=333.3 \text{ Hz}$) ACS data. T_c was identified at zero resistivity (within the noise level of $\pm 10^{-6} \Omega$) and at the point where the line drawn on the steepest part of the diamagnetic ACS curve meets the T -independent baseline associated with the negligibly small normal-state (NS) signal. T_c values obtained from these methods agree within 1 K for most of the samples.¹⁹

Patterned thin films with evaporated gold contact pads and high-density (85–95% of the theoretical density) sintered bars were used for resistivity measurements. Resistivity was measured using the four-terminal configuration. In previous studies^{4,17,19,24} we have analyzed $\rho(T, p)$ of a large number of $\text{Y}_{1-x}\text{Ca}_x\text{Ba}_2(\text{Cu}_{1-y}\text{Zn}_y)_3\text{O}_{7-\delta}$ sintered and c -axis-oriented thin films with $y \leq 0.05$ and found the pseudogap tempera-

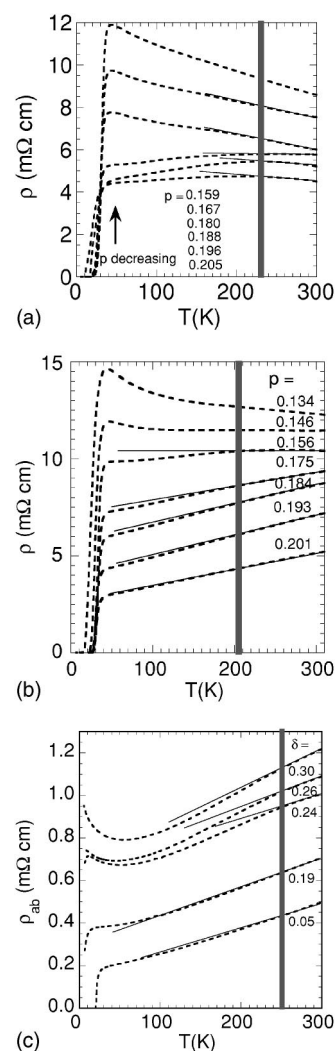


FIG. 2. Anomalous $T^*(p)$ of (a) sintered $\text{Y}_{0.80}\text{Ca}_{0.20}\text{Ba}_2(\text{Cu}_{0.94}\text{Zn}_{0.06})_3\text{O}_{7-\delta}$ (S1), (b) sintered $\text{Y}_{0.80}\text{Ca}_{0.20}\text{Ba}_2(\text{Cu}_{0.945}\text{Zn}_{0.055})_3\text{O}_{7-\delta}$ (S2), and (c) c -axis-oriented thin film of $\text{YBa}_2(\text{Cu}_{0.93}\text{Zn}_{0.07})_3\text{O}_{7-\delta}$ (from Ref. 28). Straight lines are drawn to locate T^* . The thick vertical lines show the p independence of T^* .

ture $T^*(p)$ to be independent of Zn content and independent of the crystalline state of the compound (which also implies that $T^*(p)$ does not depend on the properties of the grain boundaries). This is because $\rho(T)$ for sintered samples represents mainly the ab -plane properties, and essentially the same value of T^* is obtained from the $\rho_{ab}(T)$ data for c -axis-oriented thin films and single-crystalline compounds when they have identical values of p .^{14,17,19,24} We have also found clear indications that $T^*(p)$ vanishes at $p=0.19 \pm 0.01$ in these samples from our magnetic and transport measurements,^{14,19,24} consistent with the findings from the specific-heat measurements by Loram *et al.*^{3,23}

$\rho(T, p)$ of two heavily disordered $\text{Y}_{0.80}\text{Ca}_{0.20}\text{Ba}_2(\text{Cu}_{1-y}\text{Zn}_y)_3\text{O}_{7-\delta}$ sintered samples is shown in Fig. 2. As is standard practice,^{2,25} we have taken T^* as the temperature at which resistivity starts to fall at a faster rate with temperature than its high-temperature T -linear

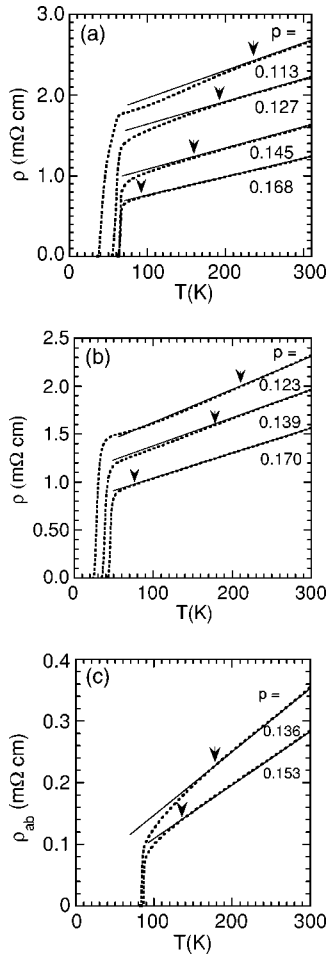


FIG. 3. Resistivity of (a) sintered $\text{Y}_{0.80}\text{Ca}_{0.20}\text{Ba}_2(\text{Cu}_{0.985}\text{Zn}_{0.015})_3\text{O}_{7-\delta}$ (b) sintered $\text{Y}_{0.80}\text{Ca}_{0.20}\text{Ba}_2(\text{Cu}_{0.96}\text{Zn}_{0.04})_3\text{O}_{7-\delta}$ and (c) c -axis-oriented $\text{Y}_{0.95}\text{Ca}_{0.05}\text{Ba}_2\text{Cu}_3\text{O}_{7-\delta}$ thin film. Straight lines are drawn to locate the pseudogap temperature T^* . Arrows mark the usual $T^*(p)$.

behavior.²⁵ It is clearly seen from Fig. 2(a) that the evolution of $\rho(T, p)$ for the first $y=0.06$ sample (S1) is different compared to other $\text{Y}_{1-x}\text{Ca}_x\text{Ba}_2(\text{Cu}_{1-y}\text{Zn}_y)_3\text{O}_{7-\delta}$ compounds with $y < 0.05$ [shown in Figs. 3]. In this (S1) sample, there is a very large residual resistivity (it violates the Mathiessen law, which predicts the residual resistivity to increase at a rate proportional to the impurity concentration, as found for samples with $y < 0.05$). Also even at fairly high hole concentration, ($p \sim 0.180$) $\rho(T)$ is nonmetallic over the whole experimental temperature range from 300 K. This may indicate significant carrier localization induced by Zn in the CuO_2 plane, but it is difficult to assess the importance of extrinsic effects, such as grain boundary resistance and the degree of porosity in the sintered sample. The most striking feature of the $\rho(T, p)$ data is the downturn in resistivity at around 230 ± 5 K, almost independent of planar hole concentration p . This downturn is somewhat masked for samples with higher oxygen deficiency (smaller p) because of the stronger nonmetallic behavior over the whole temperature range. These downturns in the $\rho(T)$ data are similar to those observed in samples with a PG [see Figs. 3]. But in this sample

it is unusual because (i) the PG-like feature is observed in resistivity for a heavily overdoped sample ($T_c=12$ K, whereas $T_{c\text{max}} \sim 27.9$ K for $y=0.06$) and (ii) T^* does not seem to change with p . The former indicates the possibility of disorder giving rise to this PG-like phenomenon, whereas the latter shows that, in such a case, this feature is almost independent of planar hole content p . In Fig. 2(b) we have shown the p -independent T^* for another heavily disordered compound (S2) from the $\rho(T)$ measurements. Although the nominal composition for S2 from a different batch was also $y=0.06$ and $x=0.20$, from the value of $T_{c\text{max}} (=32$ K) we think that the actual Zn concentration in the CuO_2 plane is a little lower, probably $\sim 5.5\%$. T^* for this sample is $\sim 205 \pm 5$ K. Several $\rho(T)$ measurements were done for these samples after each oxygen annealing, and measurements were also repeated after time intervals of several months. Each time we have observed the characteristic downturn in $\rho(T)$ at the same temperature. It is worth mentioning that for a given value of p , $\rho(T, p)$ of S1 appears to be more nonmetallic than S2. We believe this is not intrinsic, but that it is related to the different level of porosity of the samples, and likely to be governed by the difference in their densities.^{26,27} The density of S2 (5.93 gm/cc) was larger than that of S1 (5.61 gm/cc). This is also supported from the values of $T_{c\text{max}}$ of the samples that are well explained by the small difference in the actual levels of Zn in the CuO_2 planes. Extrinsic properties, such as the conductivity at grain boundaries, can have a large effect on $\rho(T)$ without having a noticeable effect on T_c .^{17,27}

To explore the matter further, we have searched the existing literature extensively to find published transport data on heavily Zn-substituted samples as a function of carrier concentration. Data with more than 5% Zn are rare, and when available, $\rho(T)$ measurements were often not done over a wide enough range of hole concentrations. We have found one source of published data²⁸ where $\rho(T)$ was measured over a wide range of p values for samples with $y=0.07$. In that study measurements were performed on high-quality c -axis-oriented thin films of $\text{YBa}_2(\text{Cu}_{1-y}\text{Zn}_y)_3\text{O}_{7-\delta}$. We show the in-plane resistivity, $\rho_{ab}(T)$,²⁸ for $\text{YBa}_2(\text{Cu}_{0.93}\text{Zn}_{0.07})_3\text{O}_{7-\delta}$ in Fig. 2(c). A p -independent T^* is seen again at 250 ± 5 K. From the reported²⁸ values of oxygen deficiencies and from the $S[290$ K] versus δ data of Zn-substituted Y123,¹⁶ we estimate the hole concentrations to be in the range $p = 0.17-0.11$ (within ± 0.01) for this film. At this point it is important to note that resistivity of this crystalline thin film is not affected because the presence of significant grain boundary resistance, the residual resistivity is much lower, and the tendency toward carrier localization is also reduced. This illustrates the role played by Zn as the principal source of disorder giving rise to the appearance of this PG-like feature in these samples. It also appears that T^* in these heavily disordered samples is determined by the amount of Zn in the CuO_2 plane. For example, we have $T^* = 205 \pm 5$ K, 230 ± 5 K, and 250 ± 5 K for samples with $\sim 5.5\%$ Zn, 6% Zn, and 7% Zn, respectively. However, $\rho(T)$ of 4% Zn substituted samples shows the usual $T^*(p)$ behavior as was found for the Zn-free samples [see Fig. 3(b)]. This shows that the presence of a disorder-induced PG temperature is a nonlinear function

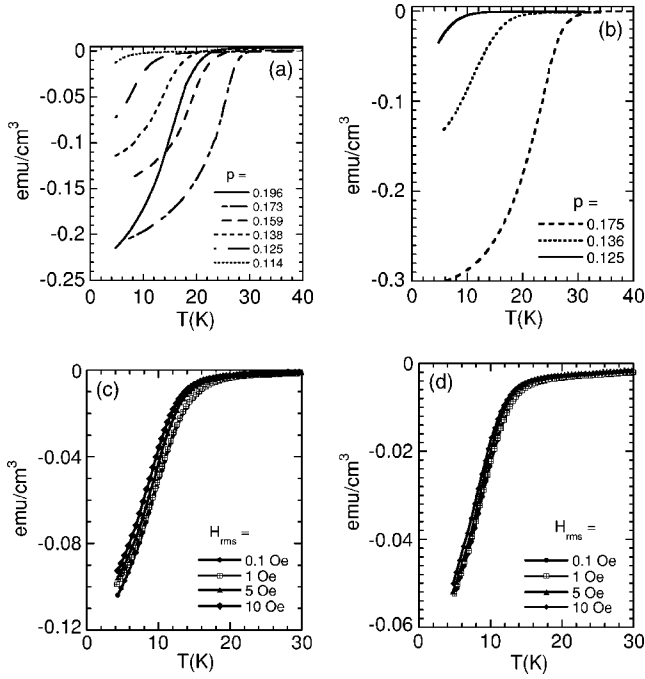


FIG. 4. (a) Low-field ($H_{rms}=0.1$ Oe) ACS of sintered S1 as a function of p , (b) low-field ACS of sintered S2 as a function of p , (c) field dependence of the ACS of sintered S1 ($p=0.205\pm 0.004$), and (d) field dependence of the ACS of powdered S1 ($p=0.205\pm 0.004$).

of Zn concentration and, at least in the $\rho(T)$ measurements, it reveals itself only in the highly disordered state. We discuss the possible implications and origins of this anomalous PG in Sec. III.

The AC susceptibility (ACS) (expressed in emu/cm³) for both S1 and S2 is shown as a function of p and magnetic field in Fig. 4. Once again quite different features are seen for these two samples compared with other sintered $Y_{1-x}Ca_xBa_2(Cu_{1-y}Zn_y)_3O_{7-\delta}$ samples with $y \leq 0.05$ (see Fig. 5). First, the magnitude of the low-field ACS signal at low- T is largely reduced for the $y > 0.05$ samples and shows a strong p dependence, namely, the ACS signal reduces rapidly with the decrease of hole content in the UD side. Both these features are absent for other samples for up to 5%Zn concentration [see Figs. 5(a) and 5(b)]. Second, the field-dependent ACS as a function of temperature shows the same qualitative features for both the sintered pellet and powder for S1 [see Figs. 4(c) and 4(d)], showing the absence of any coupling T_c and also the absence of any intergrain contribution to the shielding current. The reduction in the normalized ACS in a powdered sample simply implies that the mean grain size is further reduced by a factor ~ 1.4 because of grinding. The rapid reduction of the low-field ACS with increasing underdoping in S1 and S2 suggests that the superconducting volume fraction decreases rapidly with decreasing hole concentration (i.e., the London penetration depth increases rapidly); whereas for a less disordered sample [Fig. 5(c)], the field-dependent ACS clearly shows the intergrain-shielding component and the grain-coupling temperature ($T_{coupling}$).²⁹

Zn is believed to destroy superconductivity on a local scale (of the order of in-plane superconducting coherence

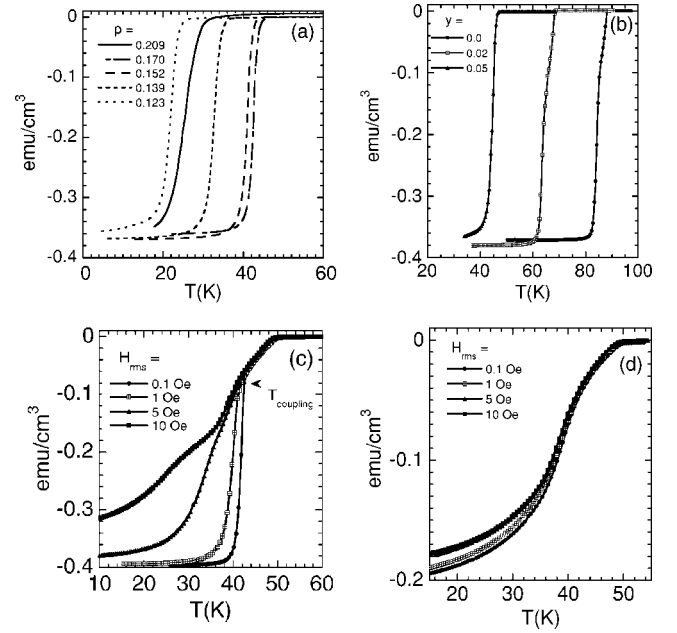


FIG. 5. (a) Low-field ACS of sintered $Y_{0.80}Ca_{0.20}Ba_2(Cu_{0.96}Zn_{0.04})_3O_{7-\delta}$ as a function of p , (b) low-field ACS of sintered $Y_{0.95}Ca_{0.05}Ba_2(Cu_{1-y}Zn_y)_3O_{7-\delta}$ with different amounts of Zn ($p=0.192\pm 0.005$ for these samples), (c) field dependence of the ACS of sintered $Y_{0.90}Ca_{0.10}Ba_2(Cu_{0.97}Zn_{0.03})_3O_{7-\delta}$ ($p=0.196\pm 0.004$), and (d) field dependence of the ACS of powdered $Y_{0.90}Ca_{0.10}Ba_2(Cu_{0.97}Zn_{0.03})_3O_{7-\delta}$ ($p=0.196\pm 0.004$). The first inter-grain coupling temperature is shown in (c).

length ξ_{ab}).^{16,30} This seems to agree with ACS data for up to 5%Zn substitution where the low-field bulk ACS signal at low-temperature showed little variation with Zn. It is possible that for heavily Zn-substituted samples the effect is not local any more and some kind of phase segregation (between superconducting and nonsuperconducting regions) over a *macroscopic* length scale takes place. The superfluid density in these highly disordered samples can be extremely low³¹ and this might facilitate this phase segregation. At temperatures near T_c , the temperature derivative of the ACS signal for the powdered samples (isolated grains) can be used to estimate the zero-temperature superfluid density, n_{s0} . At $T \rightarrow T_c$, where the London penetration depth $\lambda(T) > a$, the mean grain size, the temperature derivative of the ACS can be expressed as $N[a^2 n_{s0}]/[15T_c]$,³² where N is a constant depending on the geometry of the grains. In our calculations we have assumed N and a to be the same for all samples under consideration. These are reasonable approximations because these compounds had nearly identical density and grinding of the pellets was done in exactly the same manner. We have calculated the fractional suppression in n_{s0} as a function of Zn content for 3%Zn and 6%Zn substituted samples with $p=0.20\pm 0.005$. The results are as follows, $[n_{s0}/T_c]_{y=0.03}/[n_{s0}/T_c]_{y=0.0}=0.48$ and $[n_{s0}/T_c]_{y=0.06}/[n_{s0}/T_c]_{y=0.0}=0.07$. Thus, n_{s0}/T_c for the 6%Zn sample is reduced to just 7% of its value for the Zn-free case at the same hole content. Whereas n_{s0}/T_c for the 3%Zn sample is reduced to 48% of its value for the Zn-free case. The above findings agree quite well with those obtained by

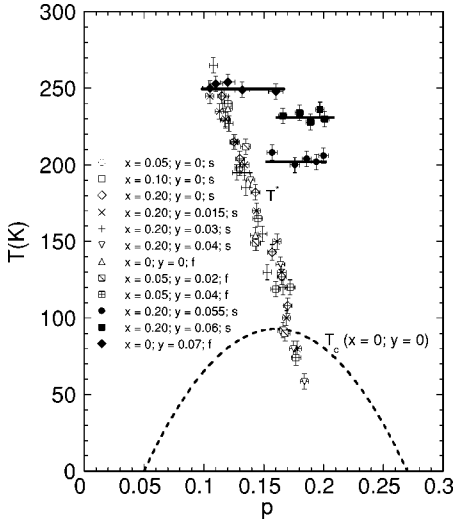


FIG. 6. The T - p phase diagram. Unfilled symbols show the data from Ref. 24 [where using Zn and magnetic field to suppress T_c we have been able to track $T^*(p)$ below $T_{c0}(p)=T_c(p, x=0, y=0)$]. Filled symbols represent anomalous T^* . Straight lines are drawn as guide to the eye. The dashed line represents the $T_{c0}(p)$ of pure Y123 with $T_{cmax}=93$ K. Sintered samples are denoted by s and the c -axis thin films by f.

Panagopoulos *et al.*³¹ from their London penetration depth measurements on magnetically aligned powders (grains).

We summarize our findings regarding the PG in Fig. 6. For comparison we have also shown $T^*(p)$ for a number of $Y_{1-x}Ca_xBa_2(Cu_{1-y}Zn_y)_3O_{7-\delta}$ compounds obtained from some of our previous studies.^{14,19,24} The contrast in the evolution of $T^*(p)$ between $y > 0.05$ samples and all the other compounds is striking. For these very heavily disordered systems $T^*(p)$ is anomalous to say the least.

III. DISCUSSION

The observed PG-like features for highly disordered $Y_{1-x}Ca_xBa_2(Cu_{1-y}Zn_y)_3O_{7-\delta}$ is surprising considering the widely held belief that the energy scale of the PG is set by p , and $T^*(p)$ either falls below or merges with the $T_c(p)$ line in the OD side. In a previous magnetic susceptibility study, Cooper and Loram³³ observed a PG-like feature in fully oxygenated sintered 7% Zn-Y123, where superconductivity was almost completely suppressed with Zn. Vobornik *et al.* also observed a pseudogap in ARPES experiments for disordered optimally doped Bi-2212 single crystals.³⁴ For Bi-2212, in-plane disorder was introduced by electron irradiation and T_c was reduced from 90 to 62 K. $\rho_{ab}(T)$ was also measured but no high- T downturn in resistivity for this 62 K optimally doped Bi-2212 was found.³⁴ In the light of present results, a possible reason might be that the sample was not “sufficiently” disordered, since we also did not see any anomalous effect in our 3%, 4%, and 5% Zn samples (where T_c was suppressed by ~ 30 K, ~ 40 K, and ~ 46 K, respectively, near the optimum doping). Also Zagoulaev *et al.*³⁵ reported the resistivity data for sintered $YBa_2(Cu_{1-y}Zn_y)_3O_7$, where for the slightly overdoped (fully oxygenated), $y=0.08$ (T_c

~ 13 K) compound, a downturn in $\rho(T)$ appeared around 250 K, consistent with the present study. Note that all the previous observations of disorder induced PG were for slightly OD (Refs. 33 and 35) and optimally doped³⁴ compounds. Here we have reported this effect over a fairly wide doping range from $p=0.205$ to 0.11.

It is fair to say that there are two main effects of Zn substitution for Cu(2) in cuprates:^{4,19,28,36,37} (i) Zn tends to localize carriers in the CuO_2 plane (depending on temperature and Zn content) and (ii) it gives rise to *Curie-like magnetic moments* possibly on the four neighboring Cu sites (in the presence of short-range antiferromagnetically correlated background). Recent ⁶³Cu NMR³⁸ and inelastic neutron-scattering studies³⁹ suggest that Zn enhances the AF correlation in Y123. There is growing evidence that an AF background with short-range order does not exist in overdoped cuprates with $p > 0.19$.⁴ The situation in highly disordered samples could be different, especially if there is phase segregation, and only a very weak form of superconductivity is present. Under these circumstances Zn-induced enhancement of short-range AF correlation might be a possibility for highly disordered $Y_{1-x}Ca_xBa_2(Cu_{1-y}Zn_y)_3O_{7-\delta}$ irrespective of the hole content. It is interesting to note that both the effects of Zn substitution (enhancement of short-range AF correlation or/and carrier localization in the CuO_2 plane) can be directly linked to the existence of the pseudogap. AF fluctuation has been held widely responsible for (or at least partly contributing to) the formation of the PG by various theoretical and experimental studies.^{4,5,40,41} In another scenario, using the t-J model, strong Coulomb repulsion has been taken as responsible for both pseudogap and superconducting pairing.⁴² In the VHS scenario,⁴³ the magnitude of the pseudogap, similar to a “Coulomb-gap”⁴⁴ increases with increasing Coulombic repulsion. Disorder leads to localization of carriers and thus weakens the electrostatic screening, which, in turn, effectively increases the Coulomb interaction. As Zn plays a similar role on carrier transport in the CuO_2 planes, it can give rise to a pseudogap in the VHS scenario.

It is hard to reconcile any precursor-pairing picture with this anomalous $T^*(p)$. On the other hand, scenarios in which the PG originates from correlations that are not related and compete with superconductivity, can possibly offer an explanation. In the competing correlations scenario $T^*(p)$ and $T_c(p)$ are detrimental to each other and the growth of one is accompanied by the decrease of the other (at least in the pure compounds). Kohno *et al.*⁴⁵ have in fact shown in their theoretical analysis that disorder can indeed strengthen one competing phase (AF) significantly over the other (e.g., superconductivity).

The abrupt appearance of this anomalous PG-like feature in resistivity as a function of disorder content is indicative of some sort of threshold mechanism in action, consistent with some recent theoretical studies.^{5,46} For example, in the study by Monthoux⁵ it was shown that as quasiparticle lifetime becomes shorter (with increasing scattering by spin fluctuations), it starts to “feel” long-range magnetic order even when only short-range correlations are present. The quasiparticle mean-free path relative to the correlation length of the short-range AF order determines the size of the pseudogap.

As the quasiparticle lifetime decreases with Zn, it is possible that at a certain level of Zn in the CuO_2 plane the scattering rate becomes high enough to dominate over the more gradual p -dependent scattering. Using the Hubbard model, it was shown that a high scattering rate leads to the removal of low-energy spectral weight.⁴⁶ In this scenario the local Coulomb repulsion U is the important parameter. Heavy Zn substitution increases the scattering rate, localizes quasiparticles, and might effectively enhance U/t (where t is the nearest-neighbor hopping energy) globally. Once $U > 8t$, the pseudogap becomes insensitive to U and therefore, should not show significant p dependence.⁴⁶

Roughly speaking, the mean distance between Zn impurities l_i in the CuO_2 plane is given by $\sim r/\sqrt{z_{pl}}$, where $z_{pl} = 3y/2$ and $r \sim 3.9 \text{ \AA}$ is the distance between Cu atoms in the plane. For $y=0.06$, $l_i \sim 13 \text{ \AA}$, close to the value of the in-plane superconducting coherence length, $\xi_{ab} \sim 15 \text{ \AA}$. Also, when $l_i \sim 13 \text{ \AA}$, two in-plane Cu atoms separate a pair of Zn atoms approximately on average. This is equivalent roughly to a situation where each in-plane Cu site contains either a Zn atom or a localized magnetic moment at the neighboring Cu atoms.³⁶ According to the *swiss cheese* model proposed by Nachumi *et al.*,⁴⁷ charge carriers within an area of $\sim \pi \xi_{ab}^2$ around each Zn atom are excluded from the superfluid. Thus, when $l_i \sim \xi_{ab}$, it is possible that the effect of Zn becomes a bulk phenomenon rather than a local one at lower concentrations. This should imply that once the distance between Zn atoms becomes comparable to a certain characteristic length, abrupt changes in the various normal and superconducting state properties take place.

Another quite strong possibility is that this apparently anomalous PG is completely different and independent from its conventional counterpart. The systematic behavior of $T_c(p, y)$ (see Fig. 1), irrespective of Zn content, supports this assumption. In this situation a conventional $T^*(p)$ should still exist for highly disordered samples. Here a much stronger

resistive feature due to the anomalous PG could obscure the features associated with the conventional $T^*(p)$ which can be detected from the $\rho(T, p)$ for less disordered compounds.

IV. CONCLUSIONS

In summary, we have observed PG-like features in highly disordered $\text{Y}_{1-x}\text{Ca}_x\text{Ba}_2(\text{Cu}_{1-x}\text{Zn}_x)_3\text{O}_{7-\delta}$ compounds from resistivity measurements. Contrary to the situation for UD cuprates, the PG temperature showed almost no p dependence over a wide range of hole contents extending from the UD to the OD regions. The magnitude of this anomalous $T^*(p)$ depends only on the amount of Zn in the CuO_2 planes. Both of these indicate that the origin of this PG-like feature is in-plane disorder. The results reported in this paper lend support to the ARPES works on optimally doped Bi-2212, where spectroscopic features of the electron-irradiated disordered compound looked similar to those of UD samples.³⁴ The ACS results of our heavily disordered $\text{Y}_{1-x}\text{Ca}_x\text{Ba}_2(\text{Cu}_{1-x}\text{Zn}_x)_3\text{O}_{7-\delta}$ show the superfluid density to be extremely low. This might be responsible for a possible phase segregation into superconducting and nonsuperconducting regions over macroscopic length scales. The anomalous T^* then might be a characteristic feature of the nonsuperconducting phase.

ACKNOWLEDGMENTS

We thank J. W. Loram and C. Panagopoulos for helpful suggestions. S.H.N. acknowledges financial support from the Commonwealth Scholarship Commission (UK), Darwin College, Cambridge Philosophical Society, Lundgren Fund, and the Department of Physics Cambridge University. R.S.I. acknowledges financial support from Trinity College, Cambridge and the Cambridge Commonwealth Trust (UK).

*E-mail address: shn21@cam.ac.uk

¹B. Batlogg and C. Varma, *Phys. World* **13**, 33 (2000).

²T. Timusk and B. Statt, *Rep. Prog. Phys.* **62**, 61 (1999).

³J. W. Loram, K. A. Mirza, J. R. Cooper, W. Y. Liang, and J. M. Wade, *J. Supercond.* **7**, 243 (1994).

⁴J. L. Tallon and J. W. Loram, *Physica C* **349**, 53 (2001).

⁵P. Monthoux, *Phys. Rev. B* **68**, 064408 (2003); cond-mat/0309552 (unpublished).

⁶V. B. Geshkenbein, L. B. Ioffe, and A. I. Larkin, *Phys. Rev. B* **55**, 3173 (1997).

⁷V. J. Emery, S. A. Kivelson, and O. Zachar, *Phys. Rev. B* **56**, 6120 (1997).

⁸J. Maly, B. Janko, and K. Levin, *Phys. Rev. B* **59**, 1354 (1999).

⁹A. P. Kampf and J. R. Schrieffer, *Phys. Rev. B* **42**, 7967 (1990).

¹⁰M. Langer, J. Schmalian, S. Grabowski, and K. H. Bennemann, *Phys. Rev. Lett.* **75**, 4508 (1995).

¹¹A. V. Chubukov, D. Pines, and J. Schmalian, cond-mat/0201140 (unpublished).

¹²J. Schmalian, D. Pines, and B. Stojkovic, *Phys. Rev. Lett.* **80**,

3839 (1998).

¹³G. V. M. Williams, J. L. Tallon, R. Michalak, and R. Dupree, *Phys. Rev. B* **57**, 8696 (1998).

¹⁴S. H. Naqib, Ph.D. thesis, University of Cambridge, UK, 2003.

¹⁵H. Alloul, P. Mendels, H. Casalta, J. F. Marucco, and J. Arabski, *Phys. Rev. Lett.* **67**, 3140 (1991).

¹⁶J. L. Tallon, J. R. Cooper, P. S. I. P. N. de Silva, G. V. M. Williams, and J. W. Loram, *Phys. Rev. Lett.* **75**, 4114 (1995).

¹⁷S. H. Naqib, R. A. Chakalov, and J. R. Cooper, *Physica C* **407**, 73 (2004).

¹⁸S. D. Obertelli, J. R. Cooper, and J. L. Tallon, *Phys. Rev. B* **46**, R14928 (1992).

¹⁹S. H. Naqib, J. R. Cooper, J. L. Tallon, and C. Panagopoulos, *Physica C* **387**, 365 (2003).

²⁰M. R. Presland, J. L. Tallon, R. G. Buckley, R. S. Liu, and N. E. Flower, *Physica C* **176**, 95 (1991).

²¹J. L. Tallon, C. Bernhard, G. V. M. Williams, and J. W. Loram, *Phys. Rev. Lett.* **79**, 5294 (1997).

²²J. L. Tallon, J. W. Loram, G. V. M. Williams, J. R. Cooper, I. R.

- Fisher, J. D. Johnson, M. P. Staines, and C. Bernhard, *Phys. Status Solidi B* **215**, 531 (1999).
- ²³J. W. Loram, J. Luo, J. R. Cooper, W. Y. Liang, and J. L. Tallon, *J. Phys. Chem. Solids* **62**, 56 (2001).
- ²⁴S. H. Naqib, J. R. Cooper, J. L. Tallon, R. S. Islam, and R. A. Chakalov, *Phys. Rev. B* **71**, 054502 (2005).
- ²⁵B. Bucher, P. Steiner, J. Karpinski, E. Kaldis, and P. Wachter, *Phys. Rev. Lett.* **70**, 2012 (1993).
- ²⁶I. R. Fisher and J. R. Cooper, *Physica C* **272**, 125 (1996).
- ²⁷A. Carrington and J. R. Cooper, *Physica C* **219**, 119 (1994).
- ²⁸D. J. C. Walker, A. P. Mackenzie, and J. R. Cooper, *Phys. Rev. B* **51**, R15653 (1995).
- ²⁹R. B. Goldfarb, A. F. Clark, A. I. Bragniski, and A. J. Panson, *Cryogenics* **27**, 475 (1987).
- ³⁰S. H. Pan, E. W. Hudson, K. M. Lang, H. Eisaki, S. Uchida, and J. C. Davis, *Nature (London)* **403**, 746 (2000).
- ³¹C. Panagopoulos, J. R. Cooper, N. Athanassopoulou, and J. Chrosch, *Phys. Rev. B* **54**, R12721 (1996).
- ³²D. Shoenberg, *Superconductivity* (Cambridge University Press, Cambridge, 1954).
- ³³J. R. Cooper and J. W. Loram, *J. Phys. I* **6**, 2237 (1996).
- ³⁴I. Vobornik, H. Berger, M. Grioni, G. Margaritondo, L. Forró, and F. Rullier-Albenque, *Phys. Rev. B* **61**, 11248 (2000).
- ³⁵S. Zagoulaev, P. Monod, and J. Jegoudez, *Phys. Rev. B* **52**, 10474 (1995).
- ³⁶P. Mendels, J. Bobroff, G. Colin, H. Alloul, M. Gabay, J. F. Marucco, N. Blanchard, and G. Grenier, *Europhys. Lett.* **46**, 678 (1999).
- ³⁷R. S. Islam, M. Phil. thesis, University of Cambridge, UK, 2001.
- ³⁸M.-H. Julien, T. Fehér, M. Horvatić, C. Berthier, O. N. Bakharev, P. Ségransan, G. Collin, and J.-F. Marucco, *Phys. Rev. Lett.* **84**, 3422 (2000).
- ³⁹Y. Sidis, P. Bourges, B. Keimer, L. P. Regnault, J. Bossy, A. Ivanov, B. Hennion, P. Gautier-Picard, and G. Collin, *cond-mat/0006265* (unpublished).
- ⁴⁰H. Shimahara, Y. Hasegawa, and M. Kohmoto, *J. Phys. Soc. Jpn.* **69**, 1598 (2000).
- ⁴¹T. Sakai and Y. Takahashi, *J. Phys. Soc. Jpn.* **70**, 272 (2001).
- ⁴²B. Kyung, *cond-mat/0101063* (unpublished).
- ⁴³J. Bouvier and J. Bok, *Physica C* **341-348**, 871 (2000).
- ⁴⁴A. L. Efros and B. I. Shklovskii, *J. Phys. C* **8**, L49 (1975).
- ⁴⁵H. Kohno, H. Fukuyama, and M. Sgrist, *J. Phys. Soc. Jpn.* **68**, 1500 (1999).
- ⁴⁶David Senechal and A.-M. S. Tremblay, *cond-mat/0308625* (unpublished).
- ⁴⁷B. Nachumi, A. Keren, K. Kojima, M. Larkin, G. M. Luke, J. Merrin, O. Tchernyshov, Y. J. Uemura, N. Ichikawa, M. Goto, and S. Uchida, *Phys. Rev. Lett.* **77**, 5421 (1996).